Amorphous-crystalline phase transition during the growth of thin films: The case of microcrystalline silicon

M. Birkholz,* B. Selle, and W. Fuhs
Hahn-Meitner-Institut, Silizium Photovoltaik, Kekuléstrasse 5, D-12489 Berlin, Germany

S. Christiansen and H. P. Strunk
Universität Erlangen-Nürnberg, Werkstoffwissenschaften, Mikrocharakterisierung, Cauerstr. 6, D-91058 Erlangen, Germany

R. Reich
Fachbereich Chemie, Freie Universität Berlin, Takustr. 3, D-14195 Berlin, Germany
(Received 27 February 2001; published 1 August 2001)

Thin silicon films of varying thickness were deposited on foreign substrates by electron-cyclotron resonance chemical vapor deposition from SiH_4-H_2 mixtures at 600 K. Optical thickness measurements, Rutherford backscattering, and transmission electron microscopy reveal that a thin amorphous interlayer of some 10 nm thickness has formed upon the substrate, before the growth of a microcrystalline layer begins. The amorphous layer is found to be deposited with a higher rate than the crystalline phase. Since similar effects have been observed for a large variety of deposition techniques, the amorphous-crystalline phase transition is considered as an inherent property of the growth of thin silicon films on foreign substrates at low homologous temperatures. The change in growth mode is interpreted in terms of Ostwald's rule of stages, which predicts the evolution of film growth to proceed via a set of phases of descending metastability and nucleation rate. In applying capillarity theory a criterion is derived from the ratio of amorphous-phase and crystalline-phase nucleation rates J_a/J_c. This ratio is developed into basic thermodynamic functions and is shown to govern the formation of either the stable or metastable phase. The approach is of general validity for thin-film deposition processes. In the case of microcrystalline silicon, experimental measures can be derived from the developed model to directly design the evolution of film structure.

DOI: 10.1103/PhysRevB.64.085402 PACS number(s): 64.60.My, 81.15.Aa, 82.60.Nh

INTRODUCTION

The growth of thin films at low temperatures is associated with a variety of morphological and structural peculiarities. Among these phenomena are the increase of density with increasing thickness, initial amorphous layers, or pronounced columnar structures.[1–3] In the case of the preparation of intentionally crystalline silicon films from silane-hydrogen mixtures an amorphous interlayer has often been observed to occur for depositions at low temperatures of about $T \leqslant 850$ K. Before the growth of the crystalline *c*-Si phase began, a layer of amorphous silicon *a*-Si was formed directly on the substrate. The phenomenon was observed for a large variety of chemical-vapor deposition (CVD) processes, such as plasma-enhanced CVD (PECVD),[4–9] very-high-frequency (VHF) PECVD,[10,11] electron-cyclotron resonance (ECR) CVD,[12] and hot-wire (HW) CVD.[13,14] In most cases the phase transition was observed for depositions on foreign substrates such as fused silica, bare and metallized glass, or oxidized Si wafers. Thus, it is of importance for applications in large-area electronics, where devices such as solar cells[15] or thin-film transistors should be configured on glass or other low-cost substrates. Some electronic devices are being developed, for which the *a*-Si/*c*-Si heterojunction is of direct relevance for its function,[16] and there is also a growing interest in phase mixtures of *a*-Si and *c*-Si preferably deposited at temperatures $T \leqslant 500$ K (Refs. 11, 17, and 18) that may exhibit new and interesting properties such as improved stability against light exposure. For applications of thin polycrystalline Si films, however, the formation of an *a*-Si interlayer is generally undesired, since the charge carrier mobility in the amorphous phase is low in comparison to *c*-Si (Ref. 19) and a band discontinuity would be introduced via the formation of an *a*-Si/*c*-Si heterojunction. Because of these considerations, an improved understanding of the amorphous-crystalline phase transition is required—for one reason, to avoid it, and for another reason, to directly control its occurrence.

We will present in this work the results obtained for a series of thin silicon films, for which the amorphous-crystalline phase transition was investigated by measurements of the optical thickness, by Rutherford backscattering (RBS) and by transmission electron microscopy (TEM). The phase transition will be analyzed according to Ostwald's rule of stages. This rule predicts the initial formation of metastable phases during the growth of crystals or thin solid films from a supersaturated liquid or gas phase, before the most stable phase starts to grow.[20,21] In some cases the formation of metastable phases during thin film growth has already been qualitatively interpreted in terms of Ostwald's rule, as in the Ti system[22] and the Fe-C system.[23] It thus appears very well suited to be applied to the amorphous-crystalline phase transition in thin silicon films that was so often observed in previous investigations. It will be shown in the following quantitatively that Ostwald's rule does indeed predict an initial amorphous growth to occur during the solidification of silicon from the gaseous Si-H system at low homologous temperatures.

TABLE I. Deposition time *t*, optical thickness *nd*, absolute thickness nd/n_{Si}, area density *Nd*, and the *nd*/*Nd* ratio as measured for the series of investigated samples. Values in parentheses give the estimated standard deviation from the numerical regression.

t (min)	*nd* (μm)	nd/n_{Si} (μm)	*Nd* (10^{15} cm^{-2})	*nd*/*Nd* (10^{-2} nm^3)
15	0.816(7)	0.239	930(13)	8.77(20)
30	1.47(1)	0.430	1825(12)	8.05(11)
60	2.80(1)	0.819	3592(15)	7.80(3)
120	5.38(2)	1.57	7082(15)	7.60(4)
240	10.60	3.1	14 114[a]	7.51[a]

[a]*Nd* of the thickest film is estimated from the linear extrapolation of $Nd(t)$.

EXPERIMENTAL AND RESULTS

Thin silicon films were prepared by plasma-enhanced CVD from silane-hydrogen SiH_4-H_2 mixtures. The plasma was generated by an ECR source operating with a 2.45 GHz microwave of 1000 W power that was coupled into the active region through a fused silica window. The deposition system has been described in detail previously.[24] The substrate temperature was set to 600 K, while gas flow rates amounted to 4 and 90 SCCM (standard cubic centimeters per minute) for SiH_4 and H_2, respectively, which corresponds to a hydrogen dilution $F_H=[H_2]/([SiH_4]+[H_2])$ of almost 96%. The total pressure in the deposition chamber was adjusted by a throttle valve to 0.93 Pa. The deposition parameters applied in this work were previously identified by a factorial analysis that aimed at the optimization of crystallinity as determined by Raman spectroscopy.[24] The average grain size in the polycrystalline films was determined by x-ray diffraction and TEM to be in the nanometer range.[12,24] However, we follow the usual convention to characterize the crystalline part of the thin films by the expression ''microcrystalline silicon.'' Depositions on different substrates were performed within the same run and the results of thin films on Mo-coated Corning glass and fused silica will be presented in the following.

In order to investigate the thickness *d* of prepared samples in combination with the internal structure, we measured both the optical thickness *nd* (*n* is the index of refraction) and the areal density *Nd* of silicon atoms (*N* is the number density). The first quantity was determined by Fourier-transform infrared (FTIR) reflection spectroscopy, while the latter was measured with RBS. The area density *Nd* and the optical thickness *nd* may both be determined with high accuracy. The measurement errors as obtained in this work (Table I) are maximally in the 1% percent range. While the first figure is a measure for the optoelectronic properties or the polarizability, the latter reflects the structural properties or packing density of the sample under investigation. The combination of both techniques may yield interesting information on the internal structure of thin films as has only recently been shown[25] and as will be demonstrated in this work also.

FTIR reflection spectra of samples on Mo-coated glass were measured with a Perkin Elmer 2000 spectrometer in the

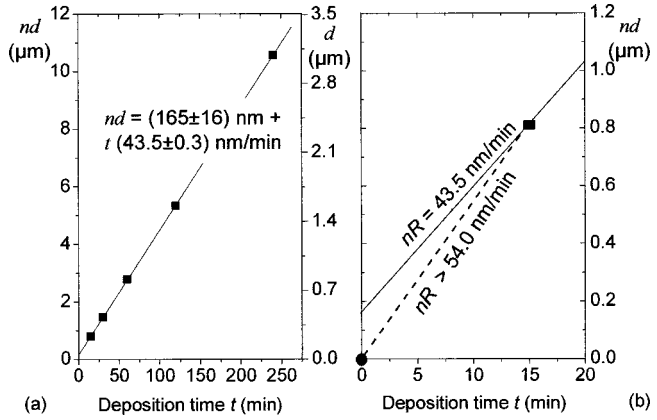

FIG. 1. Optical thickness *nd* as determined for five different thin Si films deposited on Mo-coated Corning glass vs deposition times *t*. (a) $nd(t)$ could very precisely be approximated by a linear function. (b) Magnification of the linear regression and the first data point of *nd* for the initial growth phase. The growth rate for the initial layer is seen to be larger than that for the main body of the film.

400–8000-cm^{-1} range. The optical thickness of each film was determined from the positions of interference fringes. Figure 1(a) displays the *nd* values versus deposition time *t* that were obtained for a thickness series comprising five samples; see also Table I. The measured data points could very precisely be described by the linear approximation $nd=a+bt$, with $a=165\pm16$ nm and $b=43.5\pm0.3$ nm/min. It can be concluded from $a\neq0$ that the growth kinetics at the initial stage is different from that in the higher-thickness regime. It has recently been shown by Raman spectroscopy that the initial layer in these samples consists of amorphous silicon.[12] We will therefore discuss the experimental data in terms of a two-layer model, which assumes the film to be built up from an intermediate amorphous layer (subscript *a*) adjacent to the substrate and a microcrystalline layer on top (subscript *c*). Regarding the interpretation of $nd(t)$ curves of a two-component film, it has to be noticed that both the refractive index and the growth rate may be different for the two subsequent phases, $n_a\neq n_c$ and $R_a\neq R_c$. The optical thickness will be assumed to be a linear superposition from the optical thickness of the two layers, i.e., $nd=n_aR_at_0+n_cR_c(t-t_0)$ or

$$nd=\left(n_a-n_c\frac{R_c}{R_a}\right)d_0+n_cR_ct=a+bt, \tag{1}$$

where d_0 and t_0 denote the critical values for which the phase transition occurs. The situation becomes simplified for large deposition times, $t\gg t_0$, or large thickness $d\gg d_0$. It can be seen in this limit that $nd\approx n_cR_ct$, i.e., the optical thickness is practically determined by the second phase layer and unaffected by the initial one. In consequence, n_cR_c may be derived from the *b* parameter of the linear fit. It can be seen from the enlargement of $nd(t)$ for the initial growth, Fig. 1(b), that $n_aR_a>n_cR_c$ must be valid. A numerical evaluation of these parameters became possible by the inclusion of further measurement data.

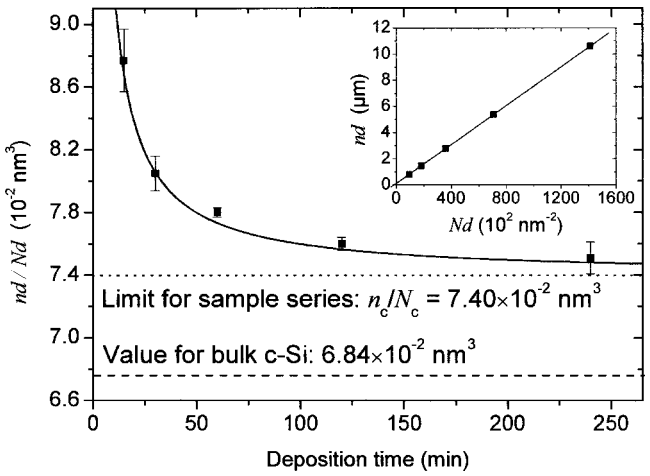

FIG. 2. Ratio of optical thickness *nd* over area density *Nd* vs deposition time *t*. The straight line shows the model function as calculated with parameters given in Table II. The inset displays the *nd* vs *Nd* function, from the slope of which n_c/N_c can be determined.

The atomic area density *Nd* of each sample of the thickness series was measured by RBS. The samples were irradiated with a total dose of 6.25×10^{13} 1.4-MeV α particles per cm^2 and measured under a detector angle of 170°. Si atom area densities were determined from the simulation of the measured spectra and the results are listed in Table I. The obtained *Nd* values as a function of deposition time could also accurately be described by a linear fit, $Nd(t)=A+Bt$, with $A=644\pm13\,\mathrm{nm}^{-2}$ and $B=585\pm2\,\mathrm{nm}^{-2}\,\mathrm{min}^{-1}$ (without figure). Again, it appeared reliable within the two-layer model to account for *Nd* by a linear superposition of *Nd* values from both layers, which yields a result analogous to Eq. (1):

$$Nd=\left(N_a-N_c\frac{R_c}{R_a}\right)d_0+N_cR_ct=A+Bt. \qquad (2)$$

Because of the separate measurement of *nd* and *Nd* for all five samples it became possible to determine also the nd/Nd ratio, which is shown in Fig. 2. A strong decrease can be realized with increasing deposition time. There is also given in the plot the value $n_{\mathrm{Si}}/N_{\mathrm{Si}}=6.84\times10^{-2}\,\mathrm{nm}^3$ as calculated for bulk-crystalline silicon. For the thinnest prepared film the nd/Nd ratio lies significantly above the *c*-Si value, from which it may be concluded that the film exhibits either a much larger index of refraction or a smaller packing density than *c*-Si or both properties. For large deposition times the difference shrinks continuously, but never approaches the *c*-Si value—even if $t,d\rightarrow\infty$. The precise limiting value can be obtained from the slope of *Nd* vs *nd*; see the inset of Fig. 2. A value of $n_c/N_c=7.40\times10^{-2}\,\mathrm{nm}^3$ is obtained for the top microcrystalline Si phase, which is 8% larger than the value for bulk-crystalline silicon. We assign this deviation in total to a deviation of the packing density $N_c=p_cN_{\mathrm{Si}}$ from the ideal *c*-Si value, i.e., $p_c=0.92$. The index of refraction is assumed to be the same as in crystalline Si, $n_c=n_{\mathrm{Si}}=3.42$, from which a deposition rate $R_c=n_cR_c/n_{\mathrm{Si}}=12.6\,\mathrm{nm/min}$ can be deduced. A packing density of 92% appears reliable, since microcrystalline Si films prepared from SiH_4-H_2 mixtures typically contain, first, hydrogen in the percent range and, second, a micronetwork of voids. Such effects are invisible to RBS and we expect both of them to contribute in comparable amounts to the lack in Si number density.

TABLE II. Physical parameters from the analysis of measured $nd(t)$ and $Nd(t)$ values in the framework of the two-layer model: refractive index *n*, packing density $p=N/N_{\mathrm{Si}}$, and growth rate *R* (in nm/min). An estimation of the critical thickness d_0 (in nm), for which the phase transition occurs, is also given.

n_c	p_c	R_c	d_0	n_a	p_a	R_a
3.42	0.92	12.7	70	4.2	0.7	22

The determination of the other physical parameters of interest, n_a, N_a, R_a and d_0, can be derived by equating the appropriate coefficients in Eqs. (1) and (2). However, the system of equations is not complete, since there are only four equations for seven quantities, and therefore the derivation of quantitative values deserves physical argumentation. The most plausible values for all physical parameters that are in accordance with the various investigations of these samples (this work and Refs. 12, 24, and 25) are compiled in Table II. According to these data, the amorphous layer is characterized by a high index of refraction, $n_a=4.2$, and a small packing density, $p_a=0.7$. The index of refraction appears large when compared with $n_{\mathrm{Si}}=3.42$. However, such large values have already been measured in *a*-Si:H; see Ref. 26. For example, an index of refraction of the same magnitude was observed for thin films prepared by argon rf sputtering under high-power conditions. The low packing density either points to a large hydrogen content or a high density of microvoids within this layer. The value obtained for d_0 will be discussed in the following section, where the results of TEM investigations will be presented. Regarding the errors of the quantities presented in Table II it is evident that there are larger errors associated with the intermediate amorphous layer than with the—much thicker—microcrystalline layer that builds up almost the total film volume. The most important source of error is related to the rough interfaces (i) on top of the film and (ii) between both silicon layers. Rough interfaces will cause a scattering of the probing ir radiation causing a systematic violation of the assumption of smooth interfaces as they are implicitly assumed by interpreting *nd* data within the appropriate formalism[27,28] of the two-layer model. Therefore, we consider the physical parameters of the microcrystalline layer more precise than those of the amorphous one. Inserting the values given in Table II into the formulaes given for *nd* and *Nd*, we are now in the position to calculate the nd/Nd model function, which is shown as a solid line in Fig. 2. The agreement between the measured data and the model function is seen to be very good. It can be concluded from these investigations that the prepared samples may be adequately described by a two-layer model. The initial growth yields an intermediate amorphous layer of some 10 nm thickness upon which a microcrystalline silicon layer is situated. Si number densities in both layers are significantly

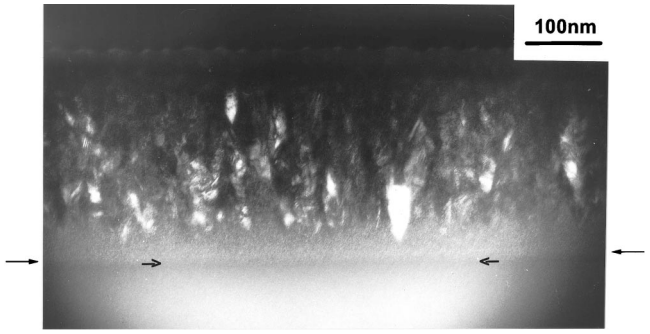

FIG. 3. Cross-sectional TEM micrograph of Si film in the vicinity of the fused silica substrate. The substrate-film interface has been marked by arrrows. The film starts to grow as an amorphous layer, from which wedge-shaped crystalline columns evolve.

smaller than in bulk-crystalline silicon, which is understood from the inclusion of microvoids and the integration of hydrogen. The deposition rate is higher for the initial amorphous phase than for the microcrystalline phase.

TEM was applied to investigate the internal structure and morphology of thin silicon films prepared under the conditions given above. For this purpose a high-resolution Philips CM300UT microscope—operated at 300 keV—was used that had a point-to-point resolution of 0.17 nm. Cross-sectional specimens were prepared conventionally by dimpling and ion milling to electron transparency in a liquid-nitrogen cooling stage. Figure 3 shows a cross-sectional micrograph that was taken from a 1.56-μm-thick Si film as deposited on a fused silica substrate. The picture displays the interfacial region close to the deposit-glass interface in dark-field contrast mode, where crystalline regions can be distinguished from amorphous regions of the layer. The growth of the crystalline layer starts from wedge-shaped cones within the amorphous interlayer. The film-substrate interface has been highlighted by small arrows. The amorphous layer at the interface had a thickness d_0 of about 30–70 nm followed by microcrystalline columnar Si growth. Due to the fact that the Si layers were deposited on glass it is difficult to determine the true edge-on orientation of the glass substrate, which would be possible in the case of a crystalline substrate. Thus the determined value of the thickness of the amorphous interlayer can just be estimated with a large error, but the result is in accordance with the estimation of the d_0 value from FTIR and RBS measurements for the set of samples deposited on Mo-coated Corning glass as presented in the previous section.

The growth mode of the crystalline part of the film is essentially columnar. Voids between the columns as often observed in the literature[10] are not pronounced. The columns were found to be mostly parallel to the growth direction or only slightly tilted with respect to each other as was visible from diffraction experiments. It has to be noted that the crystallites forming the columns are strongly twinned as is visible from intracrystalline twin lamellae that reside parallel to the interface. We conclude that the occurrence of an amorphous interlayer in this sample can clearly be stated and it was also observed for two other Si films prepared under different deposition conditions (not shown here). Although the amorphous-crystalline phase transition is well known from other chemical vapor deposition techniques like low-pressure CVD (LPCVD),[29] PECVD,[6–8,14] or hot-wire CVD,[13] its examination by TEM is novel for ECR-prepared silicon films.

DISCUSSION

Before analyzing the amorphous-crystalline phase transition, it should be mentioned that the microscopic mechanisms of amorphous and crystalline thin-film deposition from SiH_4-H_2 mixtures at low homologous temperatures by plasma-assisted CVD is not fully understood as yet. For instance, there exists no consensus about many details of the complex plasma chemistry and growth mechanisms in the solid phase. Although the understanding of certain aspects of the PECVD process has considerably improved during the last decade,[30] the state of affairs is far distinct from the theoretical insight into medium-temperature LPCVD of polycrystalline silicon, where chemical-kinetic models allow for the accurate simulation of the process; see Ref. 31 and references cited therein. We will therefore consider in the following the overall chemical reaction, $SiH_4 \leftrightarrow Si(s) + 2H_2$, for which thermodynamic functions ΔG and ΔH are well known,[32] at least for $Si(s)$ associated with crystalline silicon. The practically universal occurrence of the amorphous-crystalline phase change implies consideration of the effect as an inherent property of the growth of thin silicon films on foreign substrates. Hence, we interpret this behavior as an example for Ostwald's step rule or Ostwald's rule of stages.[20] According to this rule, the condensation of a solid phase from a supersaturated solution or gas phase first leads to the formation of metastable phases, before the most stable phase is finally condensed and continuously formed from that point.[21] During this process of structural evolution the nucleation velocity and growth velocity of the condensate decrease successively from one phase to the next phase. The amorphous silicon and microcrystalline silicon (subscripts *a* and *c*) will be associated with the metastable and stable phase, respectively. The thermodynamic quantities that govern the phase transition are the difference in free energy $\Delta G_{ca} = \Delta G_a - \Delta G_c$ and enthalpy $\Delta H_{ca} = \Delta H_a - \Delta H_c$ between amorphous and crystalline silicon, which both are positive due to the metastability of *a*-Si with respect to *c*-Si.[33,34]

Figure 4 presents a scheme for the growth of thin silicon films showing the variations of the free energy $G(r)$ of solidified grains as a function of a size parameter *r*. This energy is an extensive quantity (dimensionality *J*) and its dependence on *r* is visualized by the left-hand side ordinate in the figure. For the following considerations use has been made of capillarity theory for heterogeneous nucleation,[2] which accounts for the formation and decay of condensed clusters by the interplay between surface energy γ and free energy ΔG of the appropriate volume phase. The latter quantity is the intensive Gibb's energy specifying the difference in chemical potentials (dimensionality J/mol) and the final states for both phases are given on the right-hand side in Fig. 4. The zero level represents the starting energy associated with the SiH_4

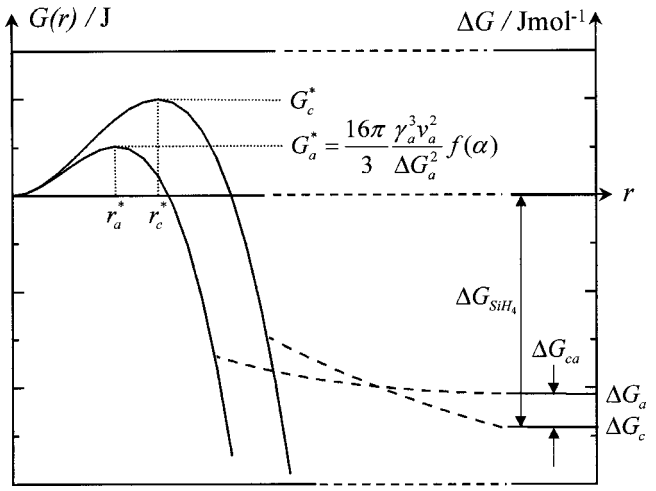

FIG. 4. Schematic drawing of the growth of silicon nuclei in the initial phase of film deposition in the framework of capillarity theory. The evolution of free energy of solidified grains is given as a function of size parameter r. A condensed cluster first has to surmount a critical free-energy barrier G^*, after which an energy gain of the chemical reaction is realized. The zero level of the ΔG axis is the Gibb's enthalpy of SiH_4. Ostwald's rule of stages predicts the metastable phase to form first (lower G^* and r^*), although the free-energy gain realized in the finally solidified film volume is smaller for the metastable phase.

precursor molecule. A condensed cluster first has to surmount a critical free-energy barrier G^*, after which an energy gain of the chemical reaction leads to the stable minimum. The solidification of silicon from SiH_4 is an exergonic reaction, such that reaction products are finally found at negative ΔG levels. The enhancement of the silane decomposition by a plasma or a hot wire has only the meaning to produce the adequate precursor molecules that will help the reaction to climb up the hill of critical cluster formation, with the detailed reaction path of it being unconsidered here. Ostwald's rule predicts the metastable phase to form first, although the free-energy gain realized in the finally solidified film volume is smaller for the metastable phase. A point of intersection must therefore appear for both $G(r)$ curves. As will be shown, amorphous nuclei are formed initially on the substrate with a higher probability, since the critical free-energy barrier G_a^* to be surmounted is smaller than for the c-Si phase, G_c^*. The same holds for the critical radii, $r_a^* < r_c^*$, which account for that size below which the clusters may disintegrate by chance. According to capillarity theory the critical free-energy barrier depends like $G^* = 16\pi\gamma^3\nu^2 f(\alpha)/3\Delta G^2$ on the surface energy γ of film clusters with respect to the vapor phase, that will be accounted for by $\gamma_{a\text{-gp}}$ and $\gamma_{c\text{-gp}}$ for the two phases under consideration with subscript gp indicating the gas-plasma phase above the silicon nuclei. The molar volume ν of amorphous and crystalline Si differ by only a few percent and will therefore be assumed to be equal for both phases. $f(\alpha)$ describes a geometrical function of the contact angle α of a nucleus with respect to the substrate plane that will be assumed to be the same for both phases. The ratio of nucleation rates J for the two phases

$$J_a/J_c = \exp[(G_c^* - G_a^*)/kT] \tag{3}$$

is of crucial importance. Here, the reliable assumption was made that the preexponential factors—accounting for the surface diffusion and desorption of precursors on the substrate—are the same for both phases. The observation of initial amorphous growth then simply implies that the probability for the formation of a-Si nuclei is much larger than for those of c-Si, or $J_a/J_c > 1$. Consequently, Eq. (3) yields the condition

$$\frac{J_a}{J_c} > 1 \Leftrightarrow (\Delta G_a/\Delta G_c)^2 > (\gamma_{a\text{-gp}}/\gamma_{c\text{-gp}})^3 \tag{4}$$

for initial amorphous growth. Regarding the left-hand side in Eq. (4), the proper Gibb's enthalpy has to be selected, which is different from the usually considered physical vapor deposition (PVD) process. For the solidification of a one-component system by PVD the value of $\Delta G = -(kT/\nu)\ln(p_{\mathrm{Si}}/p_E)$ is derived from the actual Si partial pressure p_{Si} over the equilibrium pressure p_E.[2] Here, in the case of chemical-vapor deposition of silicon from silane, the dynamic equilibrium between solid Si and the major silicon gas-phase component has to be considered. Therefore, the negative Gibb's enthalpies $-\Delta G_{\mathrm{SiH_4}}$ of SiH_4 with respect to amorphous and crystalline Si have to be inserted, and we obtained instead of Eq. (4)

$$\left(1 - \frac{\Delta G_{ca}}{\Delta G_{\mathrm{SiH_4}}}\right)^2 > \left(\frac{\gamma_{a\text{-gp}}}{\gamma_{c\text{-gp}}}\right)^3. \tag{5}$$

For the evaluation of the right-hand side of Eq. (4) use is made of the proportionality between surface energy and the heat of sublimation $(\gamma_{a\text{-gp}}/\gamma_{c\text{-gp}})^3 = (\Delta H_{a,\mathrm{sub}}/\Delta H_{c,\mathrm{sub}})^3$, which holds, if the pressure-volume product pV is small and can be neglected. Again it has to be argued that the evaluation of the $\gamma_{a\text{-gp}}/\gamma_{c\text{-gp}}$ ratio would account for the one-component PVD process, where the retransition from solidified species into the gas phase is accounted for by the heat of sublimation. In the case of the CVD process investigated here; however, the solidified silicon phase does not equilibrate with a hypothetical phase of gaseous silicon atoms, but with SiH_4 molecules. The appropriate generalization for CVD processes would accordingly be to make use of the heat of formation of SiH_4 instead of $\Delta H_{c,\mathrm{sub}}$. We, therefore, finally write condition (4) in the form

$$\left(1 - \frac{\Delta G_{ca}}{\Delta G_{\mathrm{SiH_4}}}\right)^2 > \left(1 - \frac{\Delta H_{ca}}{\Delta H_{\mathrm{SiH_4}}}\right)^3. \tag{6}$$

The negative sign in front of the fraction on the right-hand side (rhs) of Eq. (6) now stems from the fact that the heat of sublimation of a-Si is smaller than for c-Si, which is another formulation of its metastability. The thermodynamic functions ΔH_{ca} and ΔG_{ca} have already been determined by a number of workers; see Ref. 35 for some references. ΔG_{ca} values were found to vary according to whether the amorphous silicon was in the stressed state or in the relaxed state, respectively. We make use of the data of Donovan *et al.*, who estimated both functions from calorimetric measurements

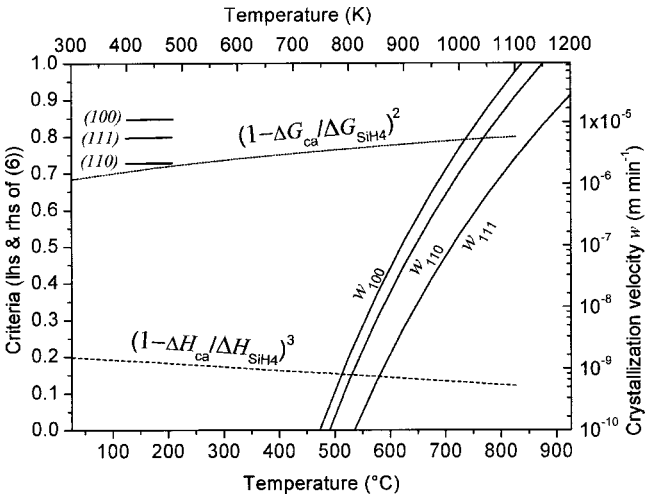

FIG. 5. Visualization of inequality (6) with lhs and rhs of Eq. (6) indicated on the left ordinate. In the framework of the presented formalism, amorphous Si nuclei can be seen to nucleate faster than crystalline ones. The figure includes the crystallization velocities w_{hkl} for the three most prominent crystallographic directions in Si, i.e., $(hkl)=(100)$, (110), and (111), that were taken from the review of Olson and Roth (Ref. 36), right ordinate. The bars indicated by different (hkl) on the left side account for $(1-\sigma_{ac}/\sigma_{hkl})^3$; the significance for the change in growth mode is outlined in the text.

during solid-phase crystallization of amorphous silicon.[33,34] Regarding the uncertainty due to the stress state of the amorphous silicon interlayer in our samples, both thermodynamic functions are given by $\Delta H_{ca}=13.4$ kJ/mol and $\Delta G_{ca}\approx 12.9$ kJ/mol with appropriate precision in the 300–1100 K temperature range. The enthalpy and free energy of SiH_4 under standard conditions $\Delta H_f^0=34.3$ kJ/mol and $\Delta G_f^0=56.9$ kJ/mol are taken from Ref. 32. Inserting the given values, it can be realized that condition (6) or $J_a/J_c>1$ is indeed satisfied. Hence, the amorphous phase would nucleate faster than the crystalline one. Criterion (6) should even hold for conditions other than only standard conditions, but its general validity shall not be investigated in this work. We have solely calculated the temperature dependence of Eq. (6), which is given in Fig. 5 and from which the validity of Eq. (6) for all relevant temperatures can be seen.

Also the transition from amorphous-to-crystalline growth and the continued formation of microcrystalline grains once after the transition has occurred may be understood within the developed concept. These effects may be motivated by the probabilistic nature of nuclei formation. During the first stages of film growth crystalline nuclei are formed with a J_c/J_a smaller probability than amorphous ones. Once the first crystalline grains are formed, however, the situation is fundamentally different for the subsequent growth process. At that stage of deposition the surface energy of newly forming nuclei equals the surface energy of that surface, on which they are deposited, and the continued formation of *c*-Si is supported. The change in growth mode will become apparent by reformulating Eq. (4). For this purpose use is made of Young's equation, $\gamma_{n\text{-gp}}=(\gamma_{s\text{-gp}}-\gamma_{ns})/\cos\alpha$, describing the mechanical equilibrium among the interfacial tensions between substrate (index *s*), nucleus (*n*), and gas phase (gp).[2]

TABLE III. Surface energies γ_{hkl} according to Ref. 29, number densities n_{hkl} and specific surface energies per atom σ_{hkl} of selected Si (hkl) surfaces.

(hkl)	(100)	(110)	(111)
γ_{hkl} (10^{-4} J cm^{-2})	2.13	1.51	1.23
n_{hkl} (10^{14} at./cm^2)	6.78	9.59	5.87
σ_{hkl} (eV/at.)	1.96	0.98	1.31

For *n* either *c* or *a* will be inserted according to whether crystalline or amorphous nuclei shall be considered. The contact angle α is approximated to become equal for both sorts of nuclei.

We now assume that first crystalline nuclei have condensed within the amorphous layer, and it will be shown that the probability for a continued crystalline growth may exceed the probability for an amorphous growth, which is identified with $J_c/J_a>1$. For analyzing the growth upon crystalline grains, the subscript *c* has to be inserted for *s* in Young's equation. If the same formalism as used for the derivation of Eqs. (4)–(6) is applied, the equivalence

$$\frac{J_c}{J_a}>1\Leftrightarrow\left(\frac{\gamma_{c\text{-gp}}-\gamma_{ca}}{\gamma_{c\text{-gp}}-\gamma_{cc}}\right)^3>\left(1-\frac{\Delta G_{ca}}{\Delta G_{SiH_4}}\right)^2 \qquad (7)$$

can be derived. This expression can now be evaluated in order to decide whether amorphous or crystalline nuclei are formed with higher probability on crystalline grains. The surface or interfacial energy between the nuclei and underlying grain will be assumed to be negligible small, $\gamma_{cc}\approx 0$. Regarding the interface energy between amorphous and crystalline silicon, the same value is used as in the theoretical modelling of solid phase crystallization, i.e., $\sigma_{ac}=0.1$ eV/at.[35] $\gamma_{c\text{-gp}}$ accounts for the surface energy of Si faces, which is well known to depend on the crystallographic orientation. The γ_{hkl} values in units of J/cm^2 for the three most prominent orientations $(hkl)=(100)$, (110), (111) according to Ref. 29 are given in Table III together with the surface number density n_{hkl} and the specific surface energy σ_{hkl} in eV/at. The ratio of surface energies, given in Eq. (7), finally reads $(1-\sigma_{ac}/\sigma_{hkl})^3$. This expression has been calculated with the values given in the table and the results are included in Fig. 5. It can be seen that criterion (7) would be fulfilled for newly formed Si nuclei upon all given surfaces, while it would not be fulfilled above a certain temperature for nuclei growing on (110) faces. The transition from amorphous-to-crystalline growth would accordingly proceed in dependence from the crystallographic faces formed, i.e., would become orientation-selective. We will not overinterpret this effect because of the limited precision of the material constants involved. It just should be noted that an orientation selection may be introduced via the ratio of surface energies and that this effect would be a consequence from the force equilibrium among the different interfaces of the nuclei, i.e., a pure mechanical phenomenon.

Since the energy gain associated with the condensation of *c*-Si surmounts that of *a*-Si, the growing nuclei occupy more and more area and even expand in the plane perpen-

dicular to the growth direction. Typical growth morphology results, built up by crystalline cones that start some dozen nanometers above the substrate and which are embedded in an amorphous matrix—as depicted in Fig. 3. Beyond a certain film thickness the interface between the gas phase and solid phase is completely composed of the crystalline phase, and solely microcrystalline silicon is formed during subsequent deposition. It has to emphasized, however, that the material constants σ_{ac} and σ_{hkl} as used in the derivation above have been determined for hydrogen-free silicon, while for the material system in our investigation, hydrogen is present in large amounts, causing all surfaces to become hydrogen-terminated. Unfortunately, the appropriate surface energies are not available yet in the case of H-terminated Si surfaces. The foregoing discussion should therefore be considered as a demonstration of the line of arguments how capillarity theory can account for a transition from amorphous-to-crystalline growth of silicon.

It furthermore may be expected that more details of the deposition process will be understood by application of the presented formalism, from which a kinetic aspect shall be mentioned. The crystallization of *a*-Si proceeds spontaneously at elevated temperatures due to its metastability, and this effect is used for the preparation of crystalline layers via solid phase crystallization.[35,36] The availability of crystalline nuclei provided, the rate-determining step of this process is the motion of the crystallization front into the amorphous phase. Parameters of the crystallization velocity $w = w_0 \exp(-E_w/kT)$ have been determined in different experiments, and the w_0 parameter has moreover been identified to vary with crystallographic orientation; for a review see Olson and Roth.[36] The physical meaning of the activation energy E_w is the mobilization of the Si-Si bond to surmount the energy barrier associated with the rearrangement into an ordered state. The set of published data indicates that the crystallization velocity in the (100) direction w_{100} enters the nm/min range at about 800 K. The crystallization velocities $w(T)$ for the three most prominent crystallographic directions have been included in Fig. 5, where $E_w = 2.8\,\mathrm{eV}$ has been inserted according to Olson and Roth.

The possibility to activate the solid-phase crystallization of amorphous silicon has important consequences for the amorphous-crystalline phase transition during the growth of thin Si films. If an amorphous interlayer would form in the critical temperature range, *in situ* crystallization of the amorphous phase—starting from the amorphous-crystalline interface and moving towards the substrate plane—would become possible during film growth. The amorphous layer would shrink more the higher the deposition temperature and the longer the deposition time after the phase transition. In an extreme case, the formation of the two-layer structure could be impeded or completely covered by the competition between amorphous deposition and *in situ* crystallization. Also the occurrence of partially *in situ* crystallized films with an upside-down layer sequence—having the amorphous phase on top of the crystalline one—would become possible by this mechanism. Such inverted layer samples have indeed been prepared by Bisaro and co-workers for LPCVD films grown at 850 K.[29] It is evident from their experiments and the foregoing considerations that the structure of Si films deposited by CVD from SiH_4 is governed by a competition between deposition rate R and crystallization velocity w. This conclusion is illustrated by Fig. 5. It can be seen from the plot that, for instance, in a typical LPCVD deposition temperature at 900 K an impractical high deposition rate R of some 100 nm/min would become necessary to avoid the crystallization front to overtake and thereby producing an amorphous silicon film. Vice versa, the LPCVD process of Si films from (non-H_2-diluted) SiH_4 may be regarded as a two-step process that is composed of the deposition of an amorphous layer and its subsequent *in situ* crystallization. As long as the design rule $R < w$ is fulfilled during the deposition this phenomenon will not be observed for the sample as investigated afterwards.

Furthermore, the effect of hydrogen dilution on the phase transition may be interpreted in terms of the proposed model. Many investigations have shown the *c*-Si phase to form preferably under high hydrogen dilutions (high F_H values),[10,13,24,37] which is assigned to the ability of hydrogen of etching away weak or strained Si-Si bonds. It may be argued within the framework of the above considerations that the nucleation rate J_a of amorphous clusters is reduced in a hydrogen-rich atmosphere, thus leading to a decreased J_a/J_c ratio. This would cause the critical thickness d_0 to shrink with increasing F_H and to become even untraceable for high F_H values. In terms of a statistical interpretation of the nucleation rate J, the same space of amorphous cluster configurations would have to be traversed in the two cases of the hydrogen-poor and hydrogen-rich gas phase. In the first case, most of the deposited Si clusters would remain on the film surface and will finally build up the two-layer film. In case of high F_H conditions, however, a large number of formed amorphous clusters would be etched back and the silicon species from which they are composed of would reevaporate into the gas phase. Films as prepared under high hydrogen dilution would accordingly be characterized not only by reduced d_0 values, but also by low deposition rates. The combination of the two phenomena has indeed been observed experimentally.[13,37] In order to deposit thin silicon films of high crystallinity within acceptable deposition times, some groups have introduced a two-step process[13] that operates under high F_H conditions initially to minimize d_0, but that switches to lower F_H values and higher deposition rates after the film growth has passed the critical thickness. We expect both mentioned effects, *in situ* crystallization and hydrogen dilution, to govern the broad variety of morphologies observed for the amorphous-crystalline phase transition in thin silicon films.

Regarding possible sources of error in the presented model, it may be argued that an analysis in terms of atomistic theories of nucleation such as the Walton-Rhodin approach[2] would have been more appropriate, since the critical clusters in the investigated temperature range would only include very few atoms. The choice in favor of capillarity theory was made because of the insufficient knowledge of the microscopic processes that act in the low-temperature deposition of thin silicon films by plasma-assisted CVD as was mentioned above. As long as these questions remain unsolved,

important parameters are missing for the application of the atomistic approach. We think that to develop a full understanding of the phenomena, the proper inclusion of atomistic and kinetic factors will clearly be needed. It is of interest, however, to realize how the capillarity approach already led to predictions in accordance with well established experimental results.

Finally, it should be pointed out that the derivation of criterion (6) is of more general validity than solely relevant for the a/c-Si system. The criterion depends on basic thermodynamic functions ΔH and ΔG of the stable phase and the metastable phase(s). The successive occurrence of metastable phases in the sequence of increasing stability is known from other material systems prepared at low homologous temperatures. A recent example is the case of the Al-O system, where it was observed for the preparation of Al_2O_3 films at 300–800 °C by pulsed magnetron sputtering that the evolution of phases during film growth proceeds in the sequence of increasing stability.[38] Many other examples were already given in the early review of the issue by Chopra.[1] The significance of Oswald's rule of stages for thin film growth has been first recognized by Buckel.[39] According to the derived criteria the driving force for the occurrence of metastable phases is due to their enhanced nucleation and growth rate. The observed sequence of increasing stable layers during film growth would then point to the evolutionary nature of the gas-solid phase transition having the fastest growing species to occur initially followed by species of slower nucleation rate but increased stability.

CONCLUSION

In conclusion, we have presented results from FTIR spectroscopy, Rutherford backscattering, and TEM on thin silicon films prepared at low homologous temperatures $\sim\frac{1}{3}T_M$ by ECR CVD. All characterization technique indicate the initial film growth to yield an amorphous silicon layer of some 10 nm thickness. A technique of analyzing the combination of optical thickness and atomic area density data has been introduced that enables the deconvolution of area density N, refractive index n and film thickness d in a double-layer system from FTIR and RBS measurement results. As a key experimental result the growth rate of the amorphous interlayer is found to surmount that of the microcrystalline top layer, although deposition conditions remained unchanged.

The amorphous-crystalline transition is proposed to be interpreted as an example for Ostwald's rule of stages, since (i) the phases are formed in the sequence of increasing stability and (ii) the nucleation velocity of metastable a-Si exceeds that of the stable c-Si phase. A criterion was derived that governs the occurrence of metastable phases during film growth, which occur because of their faster nucleation velocity. The criterion depends on basic thermodynamic functions and can easily be applied to other material systems for which these functions are known. Applying the criterion to the growth of thin silicon films, important experimental phenomena such as the effect of high hydrogen dilution can consistently be understood.

ACKNOWLEDGMENTS

We thank E. Conrad for sample preparation, and G. Keiler, J. Krause, and M. Schmidt for technical assistance. Many thanks is also due D. Aspnes and O. Nast for helpful discussions. A part of the TEM work was performed at the Central Facility for High Resolution Electron Microscopy at the University of Erlangen. This work was supported by the Bundesministerium für Wirtschaft (Contract No. 329773).

*Present address: Fraunhofer-Institut für Schicht-und Oberflächentechnik, Bienroder Weg 54E, 38108 Braunschweig, Germany.

[1] K. L. Chopra, *Thin Film Phenomena* (McGraw-Hill, New York, 1969), Chap. IV.

[2] M. Ohring, *The Materials Science of Thin Films* (Academic, San Diego, 1992), Chaps. 1 and 5.

[3] E. S. Machlin, *The Relationship Between Thin Film Processing and Structure* (Giro, Croton-on-Hudson, 1995) Chaps. 2 and 3.

[4] I. Sieber, I. Urban, I. Dörfel, S. Koynov, R. Schwarz, and M. Schmidt, Thin Solid Films **276**, 314 (1996).

[5] L. L. Smith, E. Srinivasan, and G. N. Parsons, J. Appl. Phys. **82**, 6041 (1997).

[6] E. Srinivasan and G. N. Parsons, J. Appl. Phys. **81**, 2847 (1997).

[7] B. Rezek, J. Stuchlik, A. Fejfar, and J. Kocka, Appl. Phys. Lett. **74**, 1475 (1999).

[8] C. Ross, J. Herion, and H. Wagner, J. Non-Cryst. Solids **266–269**, 69 (2000).

[9] K. Brühne, S. Klein, and M. B. Schubert, in *Proceedings of the 16th European Photovolt. Solid Energy Conference, Glasgow*, 2000 (James and James, London, 2000), VB 1.17.

[10] L. Houben, M. Luysberg, P. Hapke, R. Carius, F. Finger, and H. Wagner, Philos. Mag. A **77**, 1447 (1998).

[11] E. Vallat-Sauvain, U. Kroll, J. Meier, N. Wyrsch, and A. Shah, J. Non-Cryst. Solids **266-269**, 125 (2000).

[12] M. Birkholz, B. Selle, E. Conrad, K. Lips, and W. Fuhs, J. Appl. Phys. **88**, 4376 (2000).

[13] J. K. Rath, F. D. Tichelaar, H. Meiling, and R. E. I. Schropp, in *Amorphous and Microcrystalline Silicon Technology—1998*, edited by S. Wagner, M. Hack, H. M. Branz, R. Schropp, and I. Shimizu, Mater. Res. Soc. Symp. Proc. **507** (Materials Research Society, Pittsburgh, 1999).

[14] P. Brogueira, V. Chu, and J. P. Conde, in *Amorphous and Heterogeneous Silicon Thin Films: Fundamentals to Devices—1999*, edited by H. M. Branz, R. W. Collins, H. Okamoto, S. Guha, and R. Schropp, Mater. Res. Soc. Symp. Proc. **557** (Materials Research Society, Pittsburgh, 1999).

[15] N. Wyrsch, P. Torres, M. Goerlitzer, E. Vallat, U. Kroll, A. Shah, A. Poruba, and M. Vanecek, Solid State Phenom. **67-68**, 89 (1999).

[16] F. Zignani, R. Galloni, R. Rizzoli, M. Ruth, C. Summonte, R. Pinghini, Q. Zini, P. Rava, A. Madan, and Y. S. Tsuo, in *Amorphous Silicon Technology—1996*, edited by M. Hack, E. A. Schiff, S. Wagner, A. Matsuda, and R. Schropp, Mater. Res. Soc. Symp. Proc. **420** (Materials Research Society, Pittsburgh, 1996).

[17] A. Fontcuberta i Morral, R. Brenot, E. A. G. Hamers, R. Vanderhagen, and P. Roca i Cabarrocas, J. Non-Cryst. Solids **266–269**, 48 (2000).

[18] C. Koch, M. Ito, V. Svrcek, M. B. Schubert, and J. H. Werner, in *Amorphous and Heterogeneous Silicon Thin Films—2000*, edited by R. W. Collins, H. M. Branz, S. Guha, H. Okamoto, and M. Stutzmann, Mater. Res. Soc. Symp. Proc. **609** (Materials Research Society, Pittsburgh, 2001).

[19] R. H. Bube, *Photovoltaic Materials* (Imperial College Press, London, 1988), p. 57.

[20] W. Ostwald, Z. Phys. Chem., Stoechiom. Verwandtschaftsl. **22**, 289 (1897).

[21] W. Kleber, H.-J. Bautsch, J. Bohm, and I. Kleber, *Einführung in die Kristallographie* (Verlag Technik, Berlin, 1990), pp. 204–206.

[22] J. A. Thornton, J. Vac. Sci. Technol. **11**, 666 (1974).

[23] R. S. Iskhakov, S. V. Komogortsev, S. V. Stolyar, D. E. Prokof'ev, V. S. Zhigalov, and A. D. Balaev, Pis'ma Zh. Eksp. Teor. Fiz. **70**, 727 (1999) [JETP Lett. **70**, 736 (1999)].

[24] M. Birkholz, E. Conrad, K. Lips, B. Selle, I. Sieber, S. Christiansen, and W. Fuhs, in *Amorphous and Heterogeneous Silicon Thin Films—2000*, edited by R. W. Collins, H. M. Branz, S. Guha, H. Okamoto, and M. Stutzmann, Mater. Res. Soc. Symp. Proc. **609** (Materials Research Society, Pittsburgh, 2001).

[25] W. Bohne, J. Röhrich, B. Selle, M. Birkholz, F. Fenske, W. Fuhs, J. Platen-Schwarzkopf, and P. Reinig, Mater. Res. Soc. Symp. Proc. **638**, in press 2000.

[26] R. Swanepoel, in Amorphous Silicon and its Alloys, edited by T. Searle (INSPEC, London, 1998), p. 386.

[27] H. Anders, *Thin Films in Optics* (Focal Press, London, 1967).

[28] O. Stenzel, *Das Dünnschichtspektrum* (Akademie-Verlag, Berlin, 1996).

[29] R. Bisaro, J. Maraino, N. Proust, and K. Zellama, J. Appl. Phys. **59**, 1167 (1986).

[30] *Amorphous and Microcrystalline Silicon Technology—1997*, edited by S. Wagner, M. Hack, E. A. Schiff, R. Schropp, and I. Shimizu, Mater. Res. Soc. Symp. Proc. **467** (Materials Research Society, Pittsburgh, 1997); *Amorphous and Microcrystalline Silicon Technology—1998*, edited by S. Wagner, M. Hack, H. M. Branz, R. Schropp, and I. Shimizu, Mater. Res. Soc. Symp. Proc. **507** (Materials Research Society, Pittsburgh, 1999); *Amorphous and Heterogeneous Silicon Thin Films: Fundamentals to Devices—1999*, edited by H. M. Branz, R. W. Collins, H. Okamoto, S. Guha, and R. Schropp, Mater. Res. Soc. Symp. Proc. **557** (Materials Research Society, Pittsburgh, 1999); in *Amorphous and Heterogeneous Silicon Thin Films—2000*, edited by R. W. Collins, H. M. Branz, S. Guha, H. Okamoto, and M. Stutzmann, Mater. Res. Soc. Symp. Proc. **609** (Materials Research Society, Pittsburgh, 2001); in Amorphous and Heterogeneous Silicon-Based Films 2001, edited by M. Stutzman, J. B. Boyce, J. D. Cohen, R. W. Collins, and W. Hanna, Mater. Res. Soc. Symp. Proc. 644 (Materials Research Society, Pittsburgh, 2001); and previous published volumes of Symposium A.

[31] T. Kamins, *Polycrystalline Silicon for Integrated Circuit Applications* (Kluwer Academic, Boston, 1988), Chaps. 1 and 2.

[32] M. W. Chase, J. Phys. Chem. Ref. Data Monogr. **9**, 1 (1998).

[33] E. P. Donovan, F. Spaepen, D. Turnbull, J. M. Poate, and D. C. Jacobson, Appl. Phys. Lett. **42**, 698 (1983).

[34] E. P. Donovan, F. Spaepen, J. M. Poate, and D. C. Jacobson, Appl. Phys. Lett. **55**, 1516 (1989).

[35] C. Spinella, S. Lombardo, and F. Priolo, J. Appl. Phys. **84**, 5383 (1998).

[36] G. L. Olson and J. A. Roth, Mater. Sci. Rep. **3**, 1 (1988).

[37] J.-H. Zhou, K. Ikuta, T. Yasuda, T. Umeda, S. Yamasaki, and K. Tanaka, Appl. Phys. Lett. **71**, 1534 (1997).

[38] O. Zywitzki and G. Hoetzsch, Surf. Coat. Technol. **94–95**, 303 (1997).

[39] W. Buckel, *Elektrische en Magnetische Eigenschappen van dunne Metallaagies, Brussels, 1961* (International Union of Pure and Applied Physics, 1961), p. 264.